Generation of Single Dispersion Precompensated 1-fs Pulses by Shaped-Pulse Optimized High-Order Stimulated Raman Scattering

Vladimir Kalosha,[2] Michael Spanner,[1] Joachim Herrmann,[2] and Misha Ivanov[1]

[1]*Steacie Institute for Molecular Sciences, NRC Canada, 100 Sussex Drive, Ottawa, Ontario K1A 0R6 Canada*

[2]*Max-Born-Institute, Max-Born-Strasse 2a, 12489 Berlin, Germany*

(Received 30 May 2001; published 25 February 2002)

We propose and theoretically analyze a new approach for generating and shaping 1-fs pulses. It combines the ideas of strong-field molecular optics and optimal control to manipulate light generation in a pump-probe Raman regime. Flexible phase control over the generated spectrum of about 3 eV width is achieved by controlling the input pulses and maximizing the coherence of medium excitation by adiabatically aligning molecules in the medium with a specially shaped pump pulse. The generated pulse is optimized for an output window, precompensating for its dispersion to all orders.

DOI: 10.1103/PhysRevLett.88.103901 PACS numbers: 42.65.Re, 42.50.Hz, 42.50.Gy, 42.65.Dr

There are two complementary approaches to generating sub-fs pulses. The first [1], based on high harmonics of incident pulses can produce pulses in the soft x-ray region with a duration of 100-200 attoseconds but low conversion efficiency. The second [2–4], based on using high-order stimulated Raman scattering (HSRS), promises 1-fs to subfemtosecond pulses in the visible-to-UV region with high conversion efficiency.

Phase control is both at the heart of quantum control [5] and at the very core of the attosecond pulse generation, where perfect phase synchronization of all colors across large bandwidth is necessary to create sub-fs pulses. It is also paramount for practical applications which have to deal with extreme dispersion of very short pulses: e.g., a 1-fs pulse centered at 400 nm is stretched 100 times when passing through 0.5 mm of LiF glass. This fragility of 1-fs pulses underscores the need to flexibly tune the phases of its spectral components, precompensating for dispersion to all orders. Unfortunately, both the bandwidth and the required phase shifts quickly become too large to be effectively handled by acousto-optic or spatial light modulators (SLM) [6].

Generation of dispersion precompensated 1-fs pulses is a nontrivial inverse problem. Indeed, dispersive elements after the nonlinear medium predetermine the required phases of a very broad output spectrum. For this predefined output, one must find a regime with optimized interaction length and accurate timing with respect to the medium response, such that the backward propagation of the desired output through the medium will induce perfect destructive interference of almost all colors, yielding a relatively narrow spectrum at the input.

We theoretically show how this problem can be solved and how flexible control over the phases of all colors required to produce single 1-fs pulses can be achieved by manipulating a much narrower input spectrum before the nonlinear medium. Our proposal combines the ideas for pulse compression by high-order stimulated Raman scattering [2–4] with the methods of strong-field molecular optics [7] and optimal control by pulse shaping [5]. The phase-amplitude structure of the output spectrum is controlled at the input into the Raman medium, when the spectrum is still narrow and can be effectively handled by SLMs. The pump-probe arrangement allows for independent control of both the medium response to the probe and the phase-amplitude structure of the probe. Such decoupling of the medium response from the probe's structure is crucial: the probe optimization becomes both simple and flexible, and the optimal solution of the inverse problem is robust due to the linear propagation regime for the probe.

In Fig. 1(a) a specially shaped, linearly polarized intense pump pulse with long rise time *adiabatically* aligns a gas of molecules (N_2) filling a hollow waveguide. Alignment to the electric field of the pump puts molecules into the so-called pendular eigenstates—coherent superpositions of the field-free rotor states [7]. Fast turn-off of the pump pulse nonadiabatically releases the molecules, starting their coherent free rotation [Fig. 1(b) and below]. The pump leaves behind a wake of rotations, inducing temporal modulation of the Raman polarization which implies modulation of the refractive index $n(t)$ for the probe. When a delayed weaker probe pulse is sent into the excited medium, its spectrum is broadened by the modulation of $n(t)$. The probe has a duration shorter than that of the local minima in Fig. 1(b) and is delayed to fit into one of them. Therefore, a continuous broad spectrum rather than many discrete Raman lines is generated, with a blue- or redshift depending on the pump-probe delay [4]. The desired spectral phases at the output are engineered by (i) amplitude-phase shaping of the probe at the input, (ii) selecting an appropriate excitation regime, and (iii) choosing the optimal pump-probe delay. In Fig. 1(a) the probe is tailored to a window into the vacuum chamber where experiments or measurements are done.

Our ideas draw from previous work on HSRS which demonstrated extremely broad spectra with discrete lines from far IR to the extreme UV [8,9]. References [2] showed that high-repetition train of sub-fs pulses can be obtained using *adiabatic* excitation of the medium with a properly tuned two-color cw field. Compressed pulses

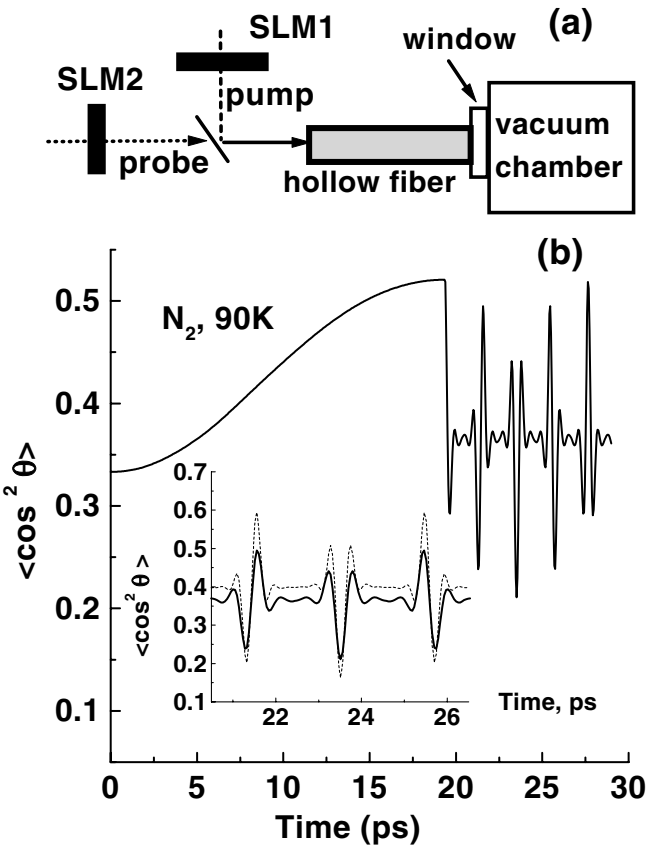

FIG. 1. (a) Schematic of our approach. The pump is shaped at SLM1 and rotationally excites N_2 molecules in the fiber. Short probe is optimally delayed and shaped at SLM2 to precompensate for dispersion ahead, including the window. (b) Averaged alignment $\langle\cos^2\theta\rangle$ of the angle between polarization and N_2 axis induced by the pump, for initial temperature $T = 90$ K and peak pump intensity $I = 1.75 \times 10^{13}$ W/cm^2. Inset: Expanded region of 21–26 ps for $I = 1.75$ (solid line) and 3.5×10^{13} W/cm^2 (dotted line).

can also be generated using short-pulse excitation in a pump-probe arrangement [3,4]. Reference [3] reported first demonstration of a train of pulses compressed to about 6 fs using *impulsive* Raman excitation first studied in [10]. Generation of single compressed pulses by HSRS is possible when the pump and the probe durations are smaller than the period of the Raman oscillations [4]. In this case their spectra remain continuous, yielding single pulses rather than high-repetition trains. This regime was used to produce the shortest (3.8 fs) single optical pulses to date [11]. There is also relation with proposals to use high-order Raman solitons [12] or plasma waves [13] for pulse compression.

The nonperturbative alignment dynamics of a homonuclear diatomic molecule in a strong laser field linearly polarized along the z axis is described by [7]

$$i\dot{\Psi}(\theta,t) = \left[\frac{\hat{J}^2}{2\mu R_{\rm eq}^2} - \frac{\alpha_\parallel\cos^2\theta + \alpha_\perp\sin^2\theta}{4}E_{\rm pu}^2(t)\right]\Psi\,. \tag{1}$$

Here $\hat{J}$ is the angular momentum operator, $R_{\rm eq}$ is the equilibrium internuclear distance, μ is the reduced mass, θ is the angle between the laser polarization (z axis) and the molecular axis, $E_{\rm pu}(t)$ is the *envelope* of the pump $\mathcal{E}_{\rm pu}(t) = E_{\rm pu}(t)\cos\omega t$, and $\alpha_\parallel(\omega)$ and $\alpha_\perp(\omega)$ are the parallel and perpendicular polarizabilities of the molecule. Equation (1) describes the evolution of an initial field-free state $|J, J_z\rangle$ into $|\Psi_{J,J_z}(\theta,t)\rangle$.

Using Eq. (1), we can find the polarization for a weak delayed probe field in a thermal ensemble, with coherent excitation of rotational states induced by the strong pump. The z component of polarization p_θ for the weak probe field of frequency ω and amplitude $\mathcal{E}_{\rm pr}(\omega)$ in a molecule aligned at an angle θ to z axis is

$$p_\theta(\omega) = [\alpha_\perp(\omega) + \Delta\alpha(\omega)\cos^2\theta]\mathcal{E}_{\rm pr}(\omega)\,, \tag{2}$$

where $\Delta\alpha = \alpha_\parallel - \alpha_\perp$. We normalize the polarizabilities to their static values, $\alpha_{\perp,\parallel}(\omega) = \alpha_{\perp,\parallel}^{(0)} f_{\perp,\parallel}(\omega)$. The functions $f_\parallel(\omega)$ and $f_\perp(\omega)$ are given by the Sellmeier-type expressions, $f(\omega) = \sum_i S_i/(1 - \omega^2/\omega_i^2)$. Below, we set $f_\parallel(\omega) \approx f_\perp(\omega) \approx f(\omega)$, with $f(\omega)$ taken from Ref. [14]. In a thermal ensemble, Eq. (1) is solved for each initial state $|J, J_z\rangle$ and then p_θ is averaged over $|\Psi_{J,J_z}(\theta,t)\rangle$ and over the initial Boltzmann distribution of $|J, J_z\rangle$. Thus, for a general probe pulse $\mathcal{E}_{\rm pr}(t)$ the polarization is

$$P(t) = N[\alpha_\perp^{(0)} + \Delta\alpha^{(0)}\langle\cos^2\theta\rangle(t)]\widehat{\rm FT}[f(\omega)\mathcal{E}_{\rm pr}(\omega)]\,. \tag{3}$$

Here N is the number density, $\langle\cdots\rangle$ implies averaging over both coherent rotational excitation and the initial Boltzmann distribution, $\widehat{\rm FT}$ means Fourier transform, and $\mathcal{E}(\omega)$ is the Fourier transform of $\mathcal{E}(t)$. The standard two-level two-photon density matrix theory for SRS [2–4] arises from Eq. (1) in the limit of only two rotational levels.

Figure 1(b) shows $\langle\cos^2\theta\rangle = \cos^2\theta(t)$ for N_2 molecules ($R_{\rm eq} \approx 1.1$ Å, $\mu = 7$ amu, $\alpha_\parallel = 17.8$ a.u., $\alpha_\perp = 10.4$ a.u.) at $T = 90$ K. Equation (1) is solved numerically for the plump pulse with adiabatic 20-ps rise, abrupt ($\ll$200 fs) fall, and peak intensities $I = 1.75$ and 3.5×10^{13} W/cm^2. This rotational excitation leads to coherent modulation of the refractive index $n(t)$ for the probe, via the $\cos^2\theta(t)$ term in Eq. (3), which contains a series of isolated rotational revivals $\sim$500 fs long (inset).

We use rotational excitation because rotations are sensitive only to the pulse envelope and are unaffected by the self-phase modulation of the pump. The adiabatic front maximizes alignment and minimizes self-phase modulation which can lead to dispersion-induced modification of the pulse front, ensuring the same alignment as the pump propagates in the medium. This aspect is in strong parallel with Refs. [2]. Rotations are negligible during the nonadiabatic end of the pump, minimizing its phase modulation and effect on rotations. Consequently, we achieve *maximum and uniform* modulation of the refractive index $n(t)$ across the medium, locked to the peak of the pump.

Hence, for propagation $\cos^2\theta(t)$ in Eq. (3) is replaced by $\cos^2\theta(t - x/v_{\rm pu})$, with $v_{\rm pu} = c/(1 + 2\pi N\chi_0)$ and $\chi_0 = (\alpha_\perp + \Delta\alpha\cos^2\theta_{\rm max})f(\omega_{\rm pu})$ the susceptibility at the peak of the pump, i.e., at maximum alignment $\cos^2\theta_{\rm max}$.

Adiabatic rise with short fall maximizes alignment during the pump and the modulation of the refractive index after. This accelerates spectral broadening and shortens the required propagation length. Deep modulation of the refractive index also traps the probe near the minimum of $n(t)$, locking it to the phase of the oscillation of $n(t)$. Indeed, for aligned molecules the probe propagates with group velocity $v \approx c/n(\omega', \cos^2\theta)$, where ω' is the current carrier frequency and $\cos^2\theta$ corresponds to the probe's position. As ω' increases, the probe keeps up with the polarization wake by sliding towards the minimum of $\cos^2\theta$, where increase of the carrier ω' stops.

The Maxwell equation for the probe pulse propagating in the hollow core fiber can be written as [15]

$$\frac{\partial \mathcal{E}_{\rm pr}}{\partial x} + \frac{1}{c}\frac{\partial \mathcal{E}_{\rm pr}}{\partial t} = -\frac{2\pi}{c}\frac{\partial P}{\partial t}. \tag{4}$$

Equation (4) does not assume the slowly varying envelope and can be used for any pulse if the refractive index is close to unity, so that the reflected wave can be included in first order only. Equation (4) is solved numerically, using Eq. (3) for medium polarization, with full dispersion in N_2 ($S_1 = 0.893, \omega_1 = 28.9$ fs^{-1}, $S_2 = 0.107, \omega_2 = 14.18$ fs^{-1}). Equation (4) ignores transverse distribution of the medium response. This is not critical, since $\cos^2\theta$ depends weakly on intensity I (see [7] and Fig. 1). Slight reduction of the alignment due to lower average pump intensity slightly increases the optimal propagation length.

To generate a 1-fs pulse after the output window, assumed to be 0.5 mm LiF glass, we optimize the pump-probe delay, the phase-amplitude structure of the probe at the input, and the propagation length L. At the input the probe must have sufficiently narrow spectrum and a smooth spectral phase, to be effectively handled in a realistic experiment. Figure 2(a) shows the electric field (solid line) and the instantaneous frequency (dotted line) before the 0.5-mm LiF window, required to obtain the transform-limited 1-fs pulse after the window [Fig. 2(a), inset]. Backward propagation through 15 cm of N_2 at $T = 90$ K and $N = 10^{20}$ cm^{-3}, for optimal pump-probe delay tuned near the third minimum in Fig. 1(b), yields the optimized input pulse as shown in Figs. 2(b)–2(d). Rotational excitation was assumed to be as shown in Fig. 1(b) for $I = 3.5 \times 10^{13}$ W/cm^2. The input pulse has a narrow spectral width of 0.1 eV and a smooth phase [see Fig. 2(c)]; the output spectrum in Fig. 2(d) gives a 1-fs pulse after the window.

The optimization can be illustrated by an approximate analytical analysis. Even though $\mathcal{E}(t)$ has a very broad spectrum, it is strongly chirped and its envelope is a slow function of time. Then the stationary phase method yields

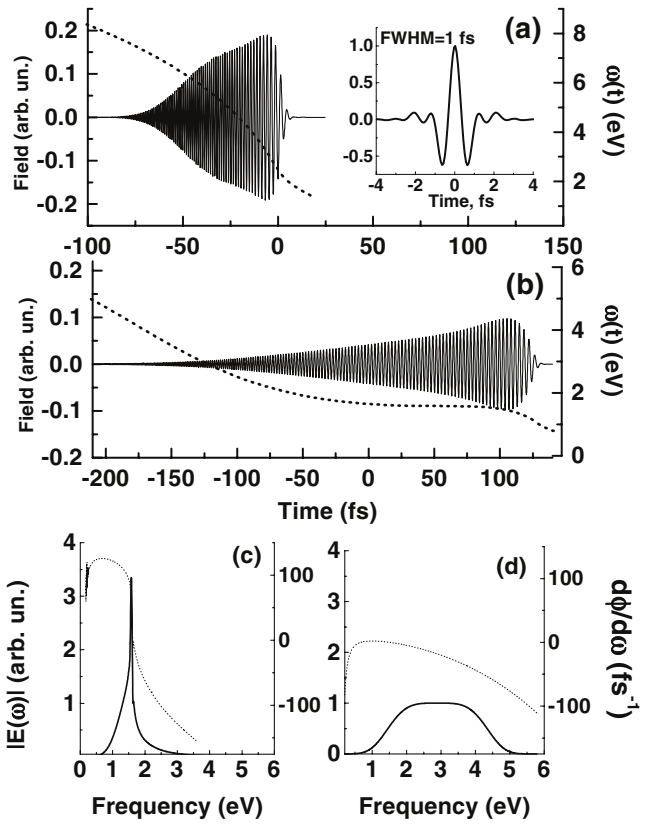

FIG. 2. Optimized compression of the probe; zero time $t = 0$ corresponds to $t = 25.62$ ps in Fig. 1(b). (a) The probe pulse before the 0.5 mm LiF output window and after it (inset), with FWHM = 1 fs. Solid line—electric field; dotted line—instantaneous frequency $\omega(t)$. (b) Required probe pulse at the input into the 15 cm hollow fiber with N_2 at 90 K and $N = 10^{20}$ cm^{-3}. (c) Corresponding probe spectrum (solid line) and delay $d\phi/d\omega$ (dotted line) at the input. (d) Output spectrum and delay before the window.

$$\widehat{\rm FT}[f(\omega)\mathcal{E}_{\rm pr}(\omega)] \approx f[\omega(t)]\mathcal{E}_{\rm pr}(t). \tag{5}$$

Here $\omega(t) = \dot{\phi}(t)$ is the instantaneous frequency of $\mathcal{E}_{\rm pr}(t) = {\rm Re}\{E_{\rm pr}(t)\exp[-i\phi(t)]\}$. With this approximation, in the moving frame $\tau = t - x/v_{\rm pu}$ Eq. (4) can be written as

$$\frac{\partial}{\partial x}\mathcal{E}_{\rm pr} = -\kappa\frac{\partial}{\partial \tau}\chi[\tau, \omega(\tau, x)]\mathcal{E}_{\rm pr}, \tag{6}$$

where $\kappa = 2\pi N/[c(1 + 2\pi N\chi_0)]$ and

$$\chi[\tau, \omega(\tau, x)] = [\alpha_\perp + \Delta\alpha\langle\cos^2\theta\rangle(\tau)]f[\omega(\tau, x)] - \chi_0. \tag{7}$$

Let the initial conditions at the input be $\phi(t, x = 0) = \phi_{\rm in}(\tau)$, $E_{\rm pr}(t, x = 0) = E_{\rm in}(\tau)$. Then the solution of Eq. (6) is

$$\phi(\tau, x) = \phi_{\rm in}[s(\tau, x)], \qquad E_{\rm pr}(\tau, x) = E_{\rm in}[s(\tau, x)]\frac{\partial s}{\partial \tau}, \tag{8}$$

where $s_{\rm in}(\tau, 0) = \tau$ and

$$\frac{\partial s}{\partial x} = -\kappa\chi[\tau, \omega(\tau, x)]\frac{\partial s}{\partial \tau}. \quad (9)$$

Since $\phi(\tau, x) = \phi_{\text{in}}[s(\tau, x)]$, the instantaneous frequency $\omega(\tau, x)$ is $\omega(\tau, x) = \omega_{\text{in}}(s)s'_\tau$, where $s'_\tau = \partial s/\partial\tau$. For sufficiently narrow input spectrum $\omega_{\text{in}}(s) \approx \omega_0$ and hence $\chi[\tau, \omega(\tau, x)] \approx \chi[\tau, \omega_0 s'_\tau]$. Substituting this into Eq. (9), we obtain a simple equation for $s(\tau, x)$ which is completely decoupled from the initial conditions $\phi_{\text{in}}, E_{\text{in}}$, except for the input carrier frequency of the probe.

Now, for a given output window, we calculate the time-dependent frequency $\omega_{\text{out}}(\tau)$ after the Raman medium, which exactly precompensates for the window dispersion. Note that $\omega_{\text{out}}(\tau)$ is defined up to an arbitrary time shift. Second, the *frequency map* $s'_\tau(\tau, L)$ is obtained by solving Eq. (9) only once. Third, we calculate the input $\omega_{\text{in}}^{(\text{opt})}(\tau) = \omega_{\text{out}}(\tau)/s'_\tau(\tau, L)$. Then, we optimize the propagation length and the time shift (and thus the pump-probe delay) by requiring that $\omega_{\text{out}}(\tau)/s'_\tau$ changes within as narrow frequency interval as possible over as long a time interval τ as possible; see Fig. 3. This ensures a large change of ω_{out}, while ω_{in} stays between the bottom two arrows in Fig. 3, which mark the input spectrum that is sufficiently narrow to be handled by an SLM. Changing the time delay results in a controlled blue- or redshift but smaller broadening (inset). Increasing L creates deep local minimum in $\omega_{\text{in}}(\tau)$ around $\tau = -130$ fs and requires a broader input spectrum, while shorter L yields less spectral broadening at the output.

If we set $\chi = u_0 \sin\Omega\tau$ (a two-level Raman medium) and neglect dispersion in the molecular medium, Eq. (9) has an exact analytical solution $\tan(\Omega s/2) = \tan(\Omega\tau/2)\exp(-\gamma L)$, where $\gamma = u_0\Omega\kappa$ [4]. Then

$$\omega_{\text{in}}^{(\text{opt})}(\tau) = \omega_{\text{out}}(\tau)[1 + \Gamma^2 + (\Gamma^2 - 1)\sin\Omega\tau]/2\Gamma, \quad (10)$$

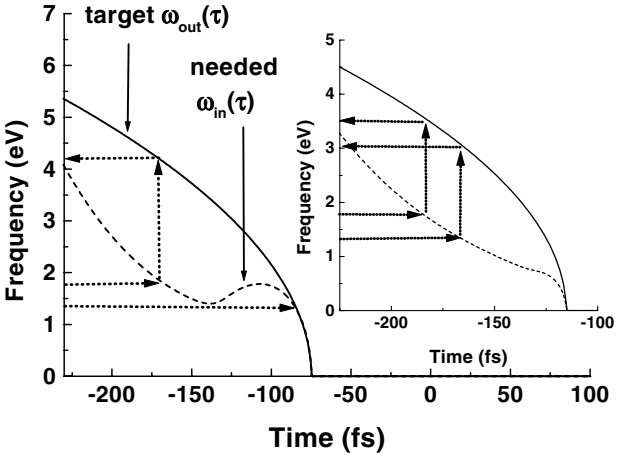

FIG. 3. Optimization procedure. Solid line—output frequency $\omega_{\text{out}}(\tau)$. Dashed line—required input $\omega_{\text{in}}(\tau) = \omega_{\text{out}}(\tau)/s'_\tau$ for $L = 15$ cm. Arrows show how a given input spectral interval 1.4–1.8 eV for $\omega_{\text{in}}(\tau)$ translates into a broad output 1.4–4.2 eV with $\omega_{\text{out}}(\tau)$ as required by the window. Reducing pump-probe delay (inset) shifts $\omega_{\text{out}}(\tau)$, resulting in the blueshift of the output 3.0–3.5 eV instead of broadening.

where $\Gamma = \exp(\gamma L)$. For a LiF-window $n^2(\omega) \approx 1 + a/(1 - \omega^2/\omega_R^2)$ with $a = 0.925\,49$ and $\omega_R = 25.4$ fs^{-1}, giving for $\omega \ll \omega_R$ the ideal output as $\omega_{\text{out}}^2(\tau) \approx \omega_R^2(T - \tau)/\tau_0$. Here $\tau_0 = 3L_{\text{glass}}a/2c\sqrt{1 + a}$ and the optimization parameter T describes an arbitrary time shift of $\omega_{\text{out}}^2(\tau)$ with respect to the polarization and determines the pump-probe delay. The optimization with these formulas gives approximately the same optimum length and delay as the numerical procedure above.

In conclusion, we have shown how active shaping of pump and probe pulses, combined with strong-field alignment of molecules, can be used to generate and shape single-cycle 1-fs pulses in the visible to UV region. Flexible control of the output spectrum has been illustrated by creating a single 1-fs pulse after the dispersive elements.

We thank P. Corkum, A. Stolow, D. Villeneuve, and M. Pshenichnikov for valuable discussions.

[1] See, e.g., M. Drescher *et al.,* Science **291**, 1923 (2001); P. M. Paul *et al.,* Science **292**, 1689 (2001).
[2] S. E. Harris and A. V. Sokolov, Phys. Rev. Lett. **81**, 2894 (1998); A. V. Sokolov *et al.,* Phys. Rev. Lett. **85**, 562 (2000).
[3] M. Wittmann, A. Nazarkin, and G. Korn, Opt. Lett. **26**, 298 (2001); Phys. Rev. Lett. **84**, 5508 (2000); A. Nazarkin and G. Korn, Phys. Rev. A **58**, 61 (1998).
[4] V. P. Kalosha and J. Herrmann, Opt. Lett. **26**, 456 (2001); Phys. Rev. Lett. **85**, 1226 (2000).
[5] See, e.g., R. S. Judson and H. Rabitz, Phys. Rev. Lett. **68**, 1500 (1992); A. Assion *et al.,* Science **282**, 919 (1998); R. Bartels *et al.,* Nature (London) **406**, 164 (2000); D. Meshulach and Y. Silberberg, Nature (London) **396**, 239 (1998).
[6] A. M. Weiner, Prog. Quantum Electron. **19**, 161 (1995); F. Verluise *et al.,* Opt. Lett. **25**, 575 (2000).
[7] See, e.g., B. Friedrich and D. Herschbach, Phys. Rev. Lett. **74**, 4623 (1995); J. J. Larsen *et al.,* Phys. Rev. Lett. **85**, 2470 (2000); M. Spanner and M. Yu. Ivanov, J. Chem. Phys. **114**, 3456 (2001), and references therein.
[8] H. Kawano, Y. Hirakawa, and T. Imasaka, IEEE J. Quantum Electron. **34**, 260 (1998); V. Schultz-von der Gathen *et al.,* IEEE J. Quantum Electron. **26**, 739 (1990); G. S. MacDonald *et al.,* Opt. Lett. **19**, 1400 (1998).
[9] See, e.g., J. Q. Liang *et al.,* Phys. Rev. Lett. **85**, 2474 (2000); F. Le Kien *et al.,* Phys. Rev. A **60**, 1562 (1999).
[10] Y. X. Yan, E. B. Gamble, and K. Nelson, J. Chem. Phys. **83**, 6391 (1985).
[11] N. Zhavoronkov and G. Korn in *Postdeadline Papers of CLEO, Baltimore, MD, 2001* (Report No. CPD19-1).
[12] A. E. Kaplan, Phys. Rev. Lett. **73**, 1243 (1994).
[13] Z. Sheng, J. Ma, and W. Yu, J. Opt. Soc. Am. B **10**, 122 (1993); V. M. Malkin, G. Shvets, and N. J. Fisch, Phys. Rev. Lett. **82**, 4448 (1999).
[14] P. E. Ciddor, Appl. Opt. **35**, 1566 (1996); B. Elden, Metrologia **2**, 71 (1966).
[15] R. K. Bullough *et al.,* Phys. Scr. **20**, 364 (1979).